Desalination and Water Treatment
www.deswater.com

1944-3994 / 1944-3986 © 2011 Desalination Publications. All rights reserved.
doi: 10.5004/dwt.2011.2674

32 (2011) 445–452
August

Arsenic removal from water using a modified rutile ore and the preliminary mechanisms

Lin Ma, Shuxin Tu*

Department of Environmental Sciences and Engineering, Huazhong Agricultural University, Wuhan 430070, China
email: stu@mail.hzau.edu.cn

Received 21 October 2010; Accepted in revised form 4 January 2011

ABSTRACT

Titanium dioxide (TiO_2) has a greater removal capacity of arsenic (As) from water, however, its practical application in water treatment is limited due to its high cost and handling difficulty. Thus, development of rutile ore (RO) (a natural ore containing titanium dioxide) as an adsorbent for As removal from water is of great significance in reducing treatment cost of As polluted water. Batch experiments were carried out to evaluate the As removal capacity of $FeCl_3$ modified RO (FMRO) and the preliminary mechanisms characterized by using scanning electron microscopy (SEM), X-ray diffraction (XRD) microanalysis, Fourier-transform infrared spectroscopy (FT-IR), and X-ray photoelectron spectroscopy (XPS). The results showed that ferric modification of RO increased As adsorption from water by 10 times over RO, and both minerals absorbed more As(V) than As(III). The As(V) and As(III) adsorption behavior of FMRO and RO could be best described by Freundlich equation. The effect of solution pH on As removal obviously presented the characteristic of parabola with a maximum around pH = 4. NaOH at concentration of 0.1 mol L^{-1} desorpted As(V) or As(III)-treated FMRO efficiently, and the regenerated FMRO could be reused. FT–IR characterization of As-treated FMRO indicated the presence of both Fe–O and As–O groups and supported the concept of surface complex formation. XPS analysis indicated that As(III) was oxidized and adsorbed in the form of As(V) on the surface of FMRO. These results explained the preliminary mechanisms of a high As absorption capacity of FMRO, and suggested that FMRO be a promising sorbent for As removal because of its ideal efficacy of As removal, rich sources of material, easy operation and handling as well as low cost.

Keywords: Rutile ore; Ferric modification; As-contaminated water; Removal percentage; Column experiments

---

1. Introduction

Arsenic has been known for centuries for its toxicity and carcinogenicity. In recent years, contamination of potable groundwater with As has become a global concern and probably poses the greatest threat to human health. In addition to naturally occurring As sources, anthropogenic As stems from industrial wastes including those from the production of pesticides and fertilizers and those from mining, smelting and agricultural production [1]. Elevated As concentrations have been found in many regions in the world, such as Greece and Hungary where hundreds of thousands of people suffered the deleterious effects on health from drinking As-contaminated water. Arsenic pollution has been reported in the USA, Mexico Laguner region, Chile and Ghana while the most alarming

---

* Corresponding author.

Presented at the Third International Conference on Challenges in Environmental Science & Engineering, CESE-2010
26 September – 1 October, 2010, The Sebel, Cairns, Queensland, Australia

exposures were in Bangladesh and India [2,3]. Recently, similar situations were found to exist in many areas of China like Shanxi, Xinjiang, Guizhou, Hubei, Guangxi, Taiwan, and Inner Mongolia where serious As pollution occurred [4–7].

The technologies for As removal include precipitation [8], ion exchange [9], membrane separation [10], oxidation [11], adsorption [12] and biological methods [13]. Although these methods have been widely employed, they have several shortcomings: high operating and waste treatment costs, high consumption of reagents and large volume of sludge formation. In contrast, adsorption methods are considered to be very important because of their treatment stability, easy operation, compact facility and regeneration capacity.

Due to easy access, low cost, efficient treatment, reliability and recoverability, environmental mineral materials have received increased attention. Using environmental mineral materials to remove As from water can take advantage of waste minerals effectively on one hand and can reduce secondary pollutants on the other. It also significantly reduces the cost and complexity of As removal treatment. Many kinds of environmental mineral materials such as bixbyite [14], goethite [15], magnetite [16], alumina [17], zero-valent iron [18], zeolite [19], quartz sand [20], fly ash [21], red mud [22–24], slag [25] and nano-titanium dioxide [26] have been developed for As removal. Those measures make recycling of waste resources possible, but also provide new affordable adsorbents for researches into environmental technology.

The ferruginous manganese ore has been successfully used for the removal of As from six real groundwater samples containing As in the range of 0.04–0.18 ppm. Arsenic removal percentages are almost 100% in all groundwater samples [27]. Titanium dioxide is also very effective for As removal from water due to its large surface area and the affinity of surface hydroxyl as well as the complex mixture of $(TiO)_2AsO_2$ and $(TiO)_2AsO$ formed on the TiO_2 surface [28]. Seida and Izumi [29] modified montmorillonite and the result showed that Cerium doped montmorillonite had a higher adsorption capacity for As. Batch studies have been performed using aluminum modified zeolites that significantly removed As(V) from water and is especially suitable for low concentration of As contaminated water [30]. There are also other modified environmental mineral materials, such as limestone which removed As from waste water through precipitation. Guo et al. [31] utilized lime–PFS method to treat As produced from sulfuric acid production, and As was removed to below 1 mg L^{-1} reaching the national emission standards. Meanwhile, some industrial wastes such as red mud, fly ash, slag, have been developed for As removal too. Kanel et al. [25] investigated the removal of As(III) from a 1 mg L^{-1} solution using slag and found that the maximum removal percentage reached 99.9%, and the maximum adsorption of As(III) was 1.40 mg g^{-1}.

It is well-known that TiO_2 is a good adsorbent of As. Bang et al. [32] found that As(V) adsorption by TiO_2 was faster than As(III) adsorption and As(III) could be directly adsorbed on TiO_2 without oxidizing As(III) into As(V). The application of nano- titanium dioxide has been demonstrated to remove 30% As(III) and 25% As(V) of an initial As concentration in 1 h [33]. Rutile ore (RO), a natural ore containing titanium, was widely used in military aviation, aerospace, marine, mechanic, chemical, and desalination because of its high strength, low specific gravity, resistance to extreme temperatures, and corrosion. As the price of RO far lower than that of titanium dioxide, it is intended to solve As pollution through the cheap RO and realize the recycling of waste resources.

Here a method is used to modify the RO with $FeCl_3$. The objectives of the present study are (1) to study the characteristic of RO and ferric modified rutile ore (FMRO); (2) to compare the As adsorption capacity and As adsorption isotherms of RO and FMRO; (3) to understand the effects of pH on As removal; (4) to investigate the desorption and regeneration of As-absorbed FMRO; (5) to illustrate the mechanisms of As removal by FMRO.

2. Materials and methods

2.1. Materials

The RO used in the study was obtained from Yingshan County, Hubei Province, China. The RO was digested by Na_2CO_3 fusion method and the chemical composition was determined by Flame atomic adsorption spectrometric method or Diantipyrglmethane photometric method (Table 1). The single-point N_2-BET method was used to measure the specific surface area of the RO sample.

The ferric modification of RO was carried out as follows: RO was grounded by high-speed universal pulverizer (Tianjin Teste Instrument Co., Ltd.), and particles below 0.149 mm were used for modification. Ten grams of the powder were added to 1 Lwater, and then 50 mL of 0.5 mol L^{-1} $FeCl_3$–$6H_2O$ was added. Finally, the mixture was stirred at 60 rpm. The resulting solution was kept for 1 d and the mixture was centrifuged at 18,300 g acceleration for 5 min. The samples of the supernatant

Table 1
Basic properties of rutile ore

	Rutile ore
Chemical composition (wt. %)	Al:32.11; Mg + Ca:26.88; Fe: 18.11; Ti:2.11
Crystals structure	Anatase
pH_{pzc}	4.91
BET surface area, m^2 g^{-1}	28.0
Average primary particle, nm	74000

were washed with deionised water until the pH reached 7 at 105°C. The FMRO was then sieved again, and the particles below 0.149 mm were used as adsorbent for the experiments.

Standard stock solution of As(V) containing 1,000 mg As L^{-1} (CB/T601-2002) was purchased from Sinopharm Chemical Reagent Co., Ltd and standard stock solution of As(III) was prepared in 18 MΩ purified water using analytical reagent As_2O_3. Test solutions containing different concentrations of As(V) and As(III) were made by diluting these stock solutions with 0.040 M NaCl solution. Each batch treatment was replicated for three times in all studies. All batch adsorption studies were done at pH 7.0 except for the experiment of pH influencing As adsorption. In all cases, the pH was adjusted using diluted HCl or NaOH as appropriate. The 50-ml sorbent/solution suspensions used for all studies were prepared in 250 ml Erlenmeyer flasks, shaken for 1 h at 180 oscillations per minute at 25°C, centrifuged at 18,300 g acceleration for 5 min, and then the samples of the supernatant were withdrawn for As analysis.

2.2. Batch experiments

The concentrations of As(V) and As(III) in the supernatant were determined using atomic fluorescence spectrometer (AFS) (Model 8220, Beijing Jitian). A mixed reagent (10% thiourea and 10% ascorbic acid) was used for pre-reduction of arsenate, and hydrochloric acid (5%) was used for hydride generation. The standard reference solution (1,000 mg L^{-1}) from Sinopharm (CB/T601-2002) was analyzed as part of the quality assurance and quality control protocol. Reagent blanks and internal standards were used, where appropriate, to ensure accuracy and precision in the AFS analysis for As.

Studies on the effect of pH, and the adsorption isotherms were done using a sorbent concentration of 20 g L^{-1} for both RO and FMRO. Except for the batch adsorption isotherms, a solution of 200 μg L^{-1} As(V) or As(III) was used in all cases due to < 200 μg L^{-1} being the As concentration of most naturally As-contaminated groundwater. The experiment for As adsorption isotherms were carried out by adding 1.0 g of RO or FMRO to 50 mL of As solution containing As(V) concentrations of 1.0–40 mg L^{-1}, or As(III) concentrations of 0.1–30 mg L^{-1}. Working solutions were adjusted to pH 4 to 10 to determine pH effects on As adsorption. Desorption experiments were carried out using 0.1 mol L^{-1} NaOH at 25°C for 24 h, and the regeneration efficiency was calculated accordingly.

2.3. Column experiments

Column experiments were performed on a laboratory scale to better simulate groundwater flow conditions and design the horizontal direction of the permeable reactive barrier (PRB). The design of the reactor is illustrated in Fig. 1. The column used was prepared with PVC of 60 cm (length) × 10 cm (width) × 10 cm (height). The perforated baffles warped by silt curtains (> 200 mesh) were placed near the two walls to prevent sand and stuffing in the reactor from being carried away. The reactor with the embedded plexiglass at the top head was free to extend, which could guarantee the whole process in anoxic conditions. Two separate columns were used for As(V) and As(III) studies. Quartz sand with a geometric size of 0.35–0.833 mm after being immersed in 1 mol L^{-1} hydrochloric acid for 24 h was filled in parts at two ends (each 1000 g), the main part of reactor was filled with 6000 g of FMRO.

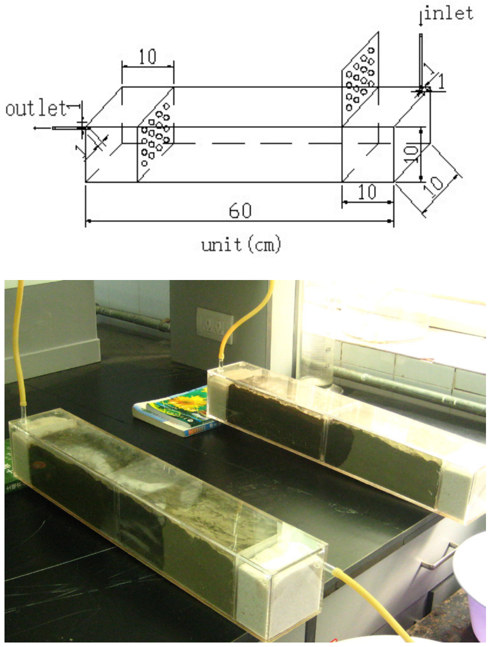

Fig. 1. Setup of a simulated column test.

Arsenic spiked water containing 500 mg L^{-1} of As(V) and As(III) (pH 7.0) was prepared for column experiments. The discharging water samples were analyzed for residual As concentration. The column was backwashed with 0.1 mol L^{-1} NaOH solution and then with distilled water after completion of one run (3 h).

2.4. Instrument analysis

X-ray diffraction (XRD) analysis was made to characterize RO and FMRO by D8 Advance X-ray Power Diffractometer (Bruker, Germany) equipped with Cu Kα radiation at a scanning speed of 2°/min from 20° to 60°, voltage of 40 kV and potential current 40 mV. The surface area of RO and FMRO was analyzed by Brunauer-Emmett-Teller (BET) method by N_2 gas adsorption at 77 K using a Quantachrome Autosorb-1 automatic surface and pore size distribution analyzer (Malvern Instruments, England). The pH_{zpc} analysis of RO and FMRO was recorded using a 90 plus Particle size analyzer Brookhaven

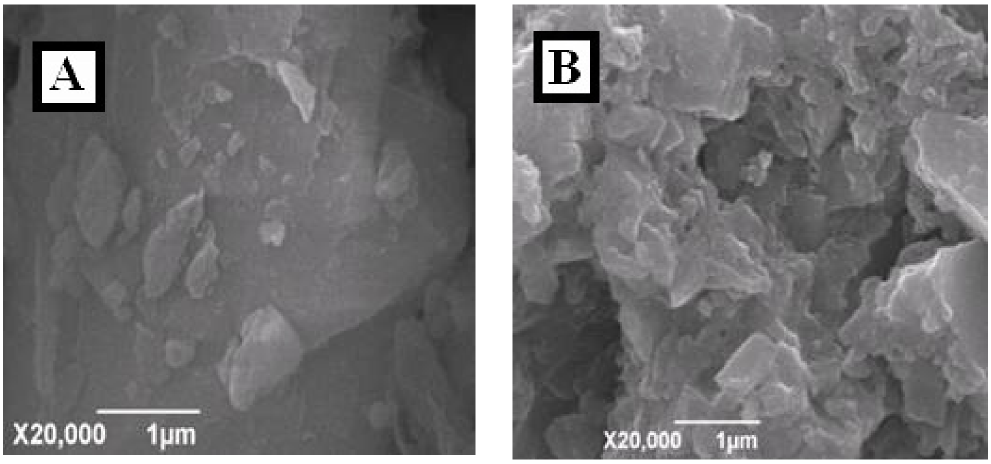

Fig. 2. High resolution electron transmission microscopic (TEM) image of two minerals with a scale bar of 1µm. (A): RO; (B): FMRO.

Zeta-Plus system (US Brookhaven Instruments Corporation). The FT-IR spectra of FMRO and As adsorbed FMRO were recorded in KBr media using a AVATAR 330 FT–IR Thermo Nicolet (German Blue Man Company). The As-adsorbed FMRO was acquired by reaction with As 100 mg/L solution with pH of 7.0 at 25°C for 1 h. Ten milligrams of the dried samples were dispersed in 200 mg of spectroscopic grade KBr to record the spectra. Forth scans were collected on each sample at a resolution of 4 cm^{-1}. The oxidation state of As on the surface of FMRO was determined by MULTILAB 2000 X-ray photoelectron spectroscopy (XPS) (Thermo Fisher Thermoelectric). The XPS pattern had a double-anode Al of 300 w and passage energy of 25 eV.

2.5. Statistical analysis

All data were the average of three replications. SigmaPlot 10.0 and Origin7.0 drawings were used to edit and draw the figures. The tables were made by MS Office 2003. Freundlich models were computed using the least square regression. Regression analysis was carried out using the SAS 8.1 software.

3. Results

3.1. Characterizations of RO and FMRO

SEM provided visual evidence for the effect of $FeCl_3$ on the RO surface erosion and collapse (Fig. 2), which showing the exterior roughening and new cavities forming after the modification process. The generation of new surface area by acidification was observed from the difference between the SEM of the RO and FMRO samples. The single-point N_2-BET method indicated that the specific surface areas of the RO and FMRO samples were about 28.0 $m^2\ g^{-1}$ and 40.0 $m^2\ g^{-1}$ respectively, which demonstrated that treatment with $FeCl_3$ increased 42.86% of the surface areas of the RO samples.

The X-ray diffraction patterns of RO and FMRO, based on the diagnostic peaks of Joint Committee for Powder Diffraction Studies database (JCPDF card 00-004-0551), demonstrated that the structure of RO was not changed by modification (Fig. 3). However, it was noteworthy that the XRD pattern obtained for FMRO presented Fe_3O_4 and γ-FeO (OH) phases corresponding to the peaks at diffraction angle (2Θ, °) values 35.67°, 56.54°, and the peak position agreed well with the Joint Committee Powder Diffraction (JCPDS) file (no. 3-863) [34]. Some irons were found to be adsorbed on the RO [34]. The pHzpc values for RO and FMRO powders were 4.91 and 4.11 respectively, indicating that FMRO had higher acidic pH_{zpc} and was mainly negatively charged (Fig. 4).

3.2. As removal and adsorption capacity of RO and FMRO

Ferric modification of RO significantly improved adsorption capacity for both As(V) and As(III) at the experimental conditions (Fig. 5). The As adsorption

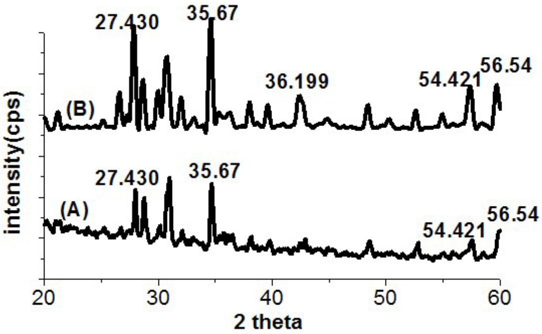

Fig. 3. XRD of RO (A) and FMRO (B).

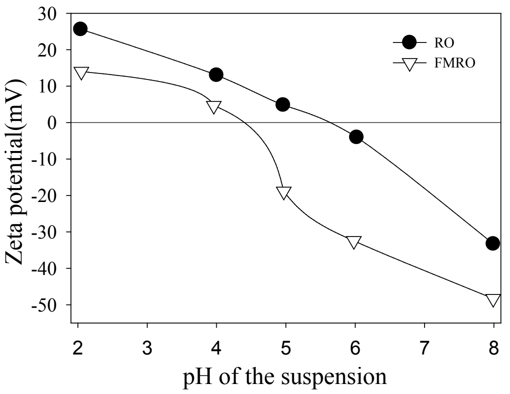

Fig. 4. Zeta-potential of RO and FMRO suspensions in 0.001 M $NaNO_3$ at different pHs.

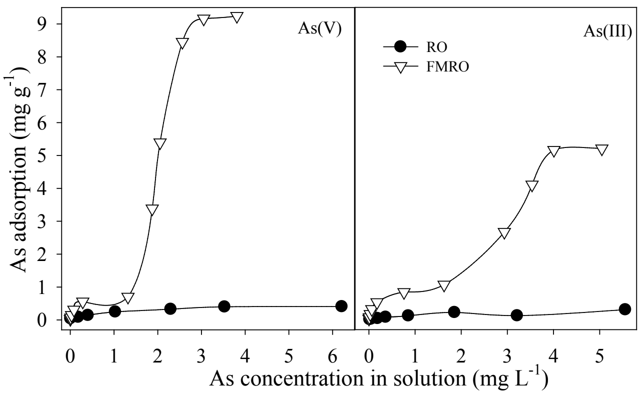

Fig. 5. Arsenic adsorption isotherms of RO and FMRO. The reaction conditions included adding 0.1 g of the adsorbents in 50 ml of As(V) or As(III) solutions at pH 7.0 and 25°C for 1 h. Each value is the mean of 3 measurements.

capacity of FMRO was 10 times greater than that of RO, with the maximum adsorption capacity of FMRO and RO being about 9.125 mg g^{-1} and 0.698 mg g^{-1} for As(V), and 5.672 mg g^{-1} and 0.524 mg g^{-1} for As(III) respectively.

Column experiments further validated the high capacity of As removal by FMRO (Fig. 6). Under the experimental conditions, when the flow of water spiked with As(V) or As(III) of 0.5 mg L^{-1} were 4.52 L and 5.47 L respectively, the As concentrations of effluent water maintained at 9.85–9.57μg L^{-1} which is lower than the As limiting standard of 10 μg L^{-1} in drinking water. When the flow of As(V) or As(III) spiked water reached 20.35 L and 24.62 L respectively, the As concentrations of effluent water still became stable and maintained at 50.10–55.51μg L^{-1} which was close to the maximum contaminant level for As in drinking water of 50 μg L^{-1}, and the removal percentages of As(V) and As(III) were both about 90%.

The Freundlich isotherm model was commonly used in fitting adsorption isotherm curve, and is expressed as: $Q_e = K_f C_e^{1/n}$, where Q_e (mg g^{-1}) is the amount of As adsorbed per gram of minerals; C_e (mg L^{-1}) is As concentration in equilibrium solution; K_f and n are two Freundlich constants. Computation by SAS 8.1 software found that the isotherms curves were well fit the Freundlich equations (Fig. 5, Table 2).

Values of n and K_f in Freundlich models reflected the reaction speed and adsorption capacity respectively, according to Thirunavukkarasu et al. [35]. Thus, Table 2 shows that the n and K_f values of FMRO were up to 1.9-fold and 11.2-fold for As(V) adsorption, and 1.5-fold and 10.9-fold for As(III) adsorption of RO respectively, suggesting that FMRO exhibited a higher As absorption speed and a greater As adsorption capacity than RO. In addition, compared to the n and K_f values of both As(V) ans(III) for the two minerals, both FMRO and RO had a higher values of n and K_f of As(V) adsorption (being 1.7-fold and 1.7-fold for FMRO respectively; being 1.3-fold and 1.7-fold for RO respectively) than those of As(III) adsorption, indicating that the two minerals exhibited the favorite of As(V) absorption.

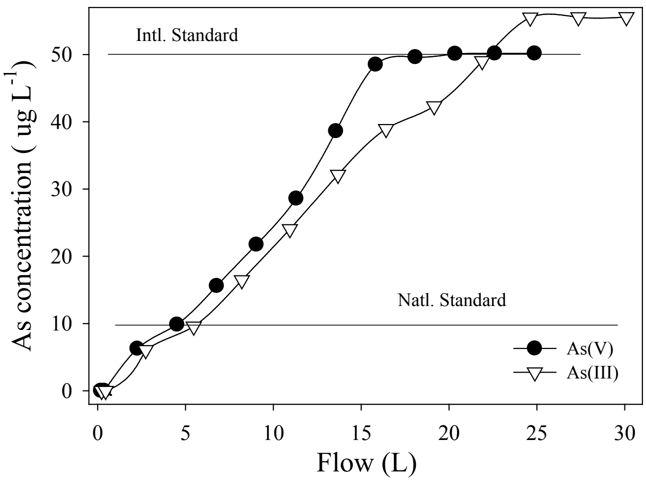

Fig. 6. Removal percentages of As(V) and As(III) from aqueous solutions by FMRO in the column experiment.

Table 2
Parameters (n and K_f) and coefficients of determination (R^2) of Freundlich model ($Q_e = K_f C_e^{1/n}$) for As adsorption isotherms of RO and FMRO (n = 8)

Crystals	As species	n	K_f	R^2
RO	As(V)	1.689	0.194	0.972*
	As(III)	1.284	0.115	0.973*
FMRO	As(V)	3.229	2.168	0.973*
	As(III)	1.927	1.258	0.987*

*Significant at $P \le 0.01$, respectively.

3.3. Effect of pH on As removal and the desorption and regeneration of As-absorbed minerals

Both FMRO and RO had a distinct maxima of As absorption around pH = 4. However, FMRO had a higher As absorption cross the solution pH of 1–10, especially at pH < 4 for As(V) absorption (Fig. 7).

Arsenic desorption percentages from As(V) or As(III)-treated FMRO by 0.1 mol L^{-1} NaOH for 24 h were 86.48% and 79.28% respectively. It was noteworthy that the regenerated FMRO could still remove 95.43% of As(V) and 94.86% of As(III) from the solution, indicating that the adsorption capacity of FMRO after regeneration was equal to the untapped FMRO (data now shown).

3.4. The mechanism of As adsorption by FMRO

FT-IR spectra of pure crystal of FMRO showed the characteristic peaks at bands of 636.26 cm^{-1} and 1629.39 cm^{-1} which was attributed to Fe–O bond extending and γ–OH or δ–OH bond bending respectively (curve *a* in Fig. 8). As(V) (curve *b* in Fig. 8) or As(III) (the curve *c* in Fig. 8)-adsorbed FMRO crystals showed bands at 959.82 cm^{-1} and 959.82cm^{-1} by $HAsO_4^{2-}$ ion stretching, bands at 894.44 cm^{-1} and 902.61 cm^{-1} by As–O–Fe stretching respectively. From the spectra by As(III)-adsorbed FMRO crystal, the bands at 1078.32 cm^{-1} and 869.92 cm^{-1} were due to As–O or $H_2AsO_4^-$ stretching and As–O or AsO_4^{3-} stretching respectively (curve *c* in Fig. 8).

Further high resolution analysis on the XPS spectra (Fig. 9) at As3d peak of FMRO indicated that the binding energies (BE) of 45.83 eV for As3d by As(V)-adsorbed FMRO corresponded to the characteristic peak position of $HAsO_4^{2-}$. The BEs of 44.7 eV, 45.3 eV, and 46.5 eV for As3d by As(III)-adsorbed FMRO were in agreement with those of $H_2AsO_4^-$, $HAsO_4^{2-}$, and AsO_4^{3-} respectively [36].

4. Discussion

Ferric modification of RO significantly improved both As adsorption capacity and As absorption speed (Fig. 5, Table 2). In our experiment, a great As adsorption capacity of FMRO was possible due to a larger surface area (40.0 $m^2 g^{-1}$) (Table 2), more fracture, new cavities and larger pore space. These results were consistent with those by Singh and Pant [17] who discovered that ferric modification of activated alumina obviously enhance As adsorption capacity, and those by Thirunavukkarasu et al. [35], Gupta et al. [37] and Kundu and Gupta [38] who reported that iron oxide-coated sand exhibited larger surface area and thus a greater As removal capacity.The FMRO in the simulated PRB experiments effectively reduced the As concentration of the initial solution to the national standards, indicating that the highly As-contaminated water could be reused through the simple adsorption process. In the meantime, the regeneration FMRO had strong adsorption capacity of As after desorption. This provided reference for the in-situ PRB's application for reuse of materials reduced economic cost, manpower, and physical resource requirement.

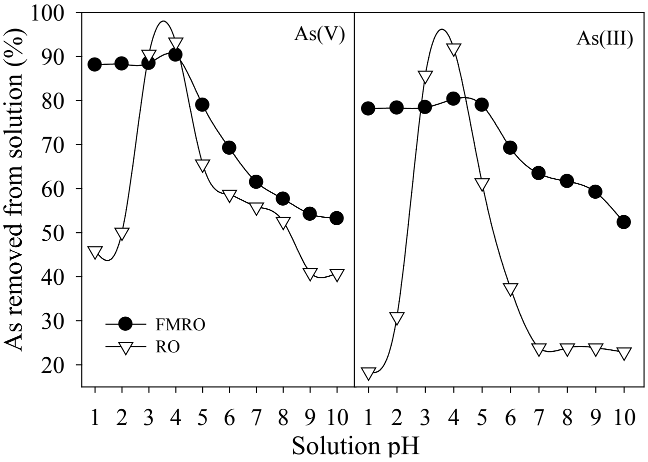

Fig. 7. Effect of solution pH on As removal after 1 h equilibration of 0.1 g RO and FMRO with 50 ml of 200 μg L^{-1} As(V) or As(III) solutions at 25°C. Each value is the mean of 3 measurements.

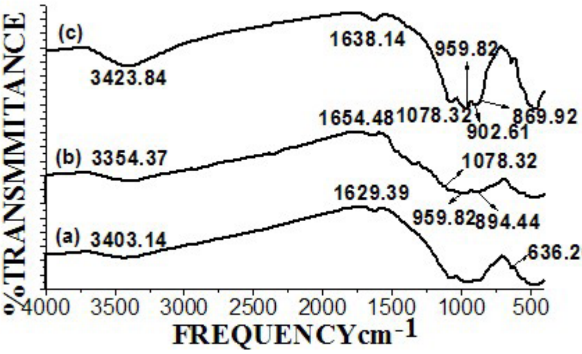

Fig. 8. The FT–IR spectra of pure or As(V) (b)/As(III) (c)-adsorbed FMRO. Line (a) stands for pure FMRO without adsorption of As(V) and As(III).

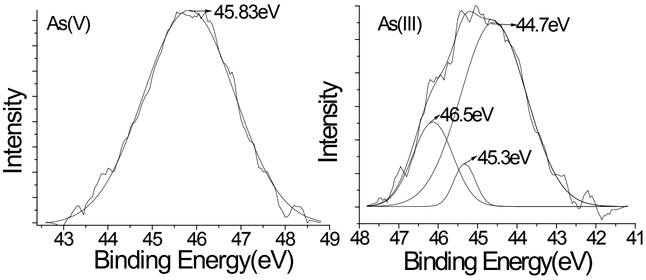

Fig. 9. The high resolution XPS at As3d peak of As(V) /As(III)-adsorbed FMRO.

It was assumed that transformation of As(III) into As(V) promoted adsorption for As by FMRO. FT-IR characterization of As-treated FMRO showed that both Fe–O and As–O groups in the minerals, and bands at 894.44 cm^{-1} and 902.61 cm^{-1} by As–O–Fe stretching were presented in As(V) or As(III)-adsorbed FMRO (curves *b*, *c* in Fig. 8). The FT–IR analysis clearly indicated that formation of $HAsO_4^{2-}$, As–O–AsO_4^{3-} and As–O–$H_2AsO_4^-$ groups in As(III)-adsorbed FMRO, which implied a possible oxidation of As(III) into As(V) in adsorption process (Fig. 8). The similar result was presented in the XPS spectra (Fig. 9), which was consistent with the results by Hsu et al. [39] who reported that reclaimed iron-oxide coated sands could be used to remove As in water. More similar studies on As absorption by ferric oxide were reported by Lakshmipathiraj et al. [15] and Goldberg and Johnston [40], who proposed that As(V) was not only bound through Fe–O bonding but also through non-surface complex As-O bonds of adsorbed As(V) species. An EXFAS studies also indicated that As(V) predominantly adsorbed on goethite was a bidendate binuclear complex and the bond was quite stable [40].

Arsenic removal was favored at lower pH values ($pH < 4$) for FMRO. This kurtosis distribution was similar to the effect of pH on As adsorption with seawater neutralized red mud [22], acid treated red mud [42,43] and sand-red mud columns [44]. Increasing As(V) adsorption with decreasing pH indicated the fewer OH-ions at lower pH conditions and thus it could compete with the As(V) anions for the available sorption sites. It was known that the predominant As(V) species existed as H_2AsO_4 and $HAsO_4^{2-}$ in the pH range of 2.2–11.5 and that the As(III) existed predominantly in form of H_3AsO_3 at $pH < 9.2$ and the $H_2AsO_3^-$ at $pH > 9.2$ [45]. Under such condition of $pH < pH_{zpc}$ ($pH_{zpc} = 4.11$), the FMRO surface was positively charged, adsorption of As(V) onto the surface of FMRO by electrically attractive reaction was expected. Only smaller adsorption force was expected between the surface of FMRO and H_3AsO_3. The surface charge of $Fe(OH)_3$ solids would become positive. The interaction between As(V) ion and $Fe(OH)_3$ was modeled by assuming ligand exchange reactions as follows:

$$\equiv M - OH + A^- + H^+ \rightleftarrows = M - A + H_2O$$

where M–OH is a surface hydroxyl group and M–A was the adsorbed species. When pH was lower than pH_{zpc}, mutual attraction between the As species and $Fe(OH)_3$ occurred.

5. Conclusion

Iron modified RO was proved to be very effective for As removal from water. The Freundlich isotherm was the best-fit adsorption isotherm model. Increment of As adsorption by ferric modification of RO was more pronounced at $pH < 4$. 0.1 mol L^{-1} NaOH could effectively desorbed As from As-treated FMRO, and the regenerated FMRO could be reused. Both XPS and FT-IR analysis suggested that As(III) was oxidized and adsorbed in the form of As(V) on the surface of FMRO, and this would be one of the main mechanisms for higher As capacity by ferric modification since FMRO absorbed more As(V) than As(III).

References

[1] Z. Lin and R.W. Puls, Adsorption, desorption and oxidation of arsenic affected by clay minerals and aging process, Environ. Geol., 39 (2000) 753–759.
[2] T.S.Y. Choong, T.G. Chuah, Y. Robiah, F.L. Gregory Koay and I. Azni, Arsenic toxicity, health hazards and removal techniques from water: an overview, Desalination, 217 (2007) 139–166.
[3] B.K. Mandal and K.T. Suzuki, Arsenic round the world: a review, Talanta, 58 (2002) 201–235.
[4] H. Guo and Y. Wang, Geochemical characteristics of shallow groundwater in Datong basin, northwestern China, J. Geochem. Exploration, 87 (2005) 109–120.
[5] P.L. Smedley, M. Zhang, G. Zhang and Z. Luo, Mobilisation of arsenic and other trace elements in fluviolacustrine aquifers of the Huhhot Basin, Inner Mongolia, Appl. Geochem., 18 (2003) 1453–1477.
[6] G. Sun, Arsenic contamination and arsenicosis in China, Toxicol, Appl. Pharmacol., 198 (2004) 268–271.
[7] Y. Zhang, M. Yang and X. Huang, Arsenic(V) removal with a Ce(IV)-doped iron oxide adsorbent, Chemosphere, 51 (2003) 945–952.
[8] S. Song, A. Lopez-Valdivieso, D.J. Hernandez-Campos, C. Peng, M.G. Monroy-Fernandez and I. Razo-Soto, Arsenic removal from high-arsenic water by enhanced coagulation with ferric ions and coarse calcite, Wat. Res., 40 (2006) 364–372.
[9] T.S. Anirudhan and M.R. Unnithan, Arsenic(V) removal from aqueous solutions using an anion exchanger derived from coconut coir pith and its recovery, Chemosphere, 66 (2007) 60–66.
[10] F. Ferella, M. Prisciandaro, I. De Michelis and F. Veglio, Removal of heavy metals by surfactant-enhanced ultrafiltration from wastewaters, Desalination, 207 (2007) 125–133.
[11] M.V. Krishna, K. Chandrasekaran, D. Karunasagar and J. Arunachalam, A combined treatment approach using Fenton's reagent and zero valent iron for the removal of arsenic from drinking water, J. Hazard. Mater., 84 (2001) 229–240.
[12] T. Tuutijarvi, J. Lu, M. Sillanpaa and G. Chen, As(V) adsorption on maghemite nanoparticles, J. Hazard. Mater., 166 (2009) 1415–1420.
[13] I.A. Katsoyiannis and A.I. Zouboulis, Application of biological processes for the removal of arsenic from groundwaters, Wat. Res., 38 (2004) 17–26.
[14] G.S. Zhang, J.H. Qu, H.J. Liu, R.P. Liu and G.T. Li, Removal mechanism of As(III) by a novel Fe–Mn binary oxide adsorbent: oxidation and sorption, Environ. Sci. Technol., 41 (2007) 4613–4619.
[15] P. Lakshmipathiraj, B.R. Narasimhan, S. Prabhakar and G. Bhaskar Raju, Adsorption of arsenate on synthetic goethite from aqueous solutions, J. Hazard. Mater., 136 (2006) 281–287.
[16] S. Yean, L. Cong, C.T. Yavuz, J.T. Mayo, W.W. Yu, A.T. Kan, V.L. Colvin and M.B. Tomson, Effect of magnetite particle size on adsorption and desorption of arsenite and arsenate, J. Mater. Res., 20 (2005) 3255–3264.
[17] T.S. Singh and K.K. Pant, Kinetics and mass transfer studies on the adsorption of arsenic onto activated alumina and iron oxide impregnated activated alumina, Wat. Qual. Res. J. Canada, 41 (2006) 147–156.

[18] S. Bang, G.P. Korfiatis and X. Meng, Removal of arsenic from water by zero-valent iron, J. Hazard. Mater., 121 (2005) 61–67.

[19] K.B. Payne and T.M. Abdel-Fattah, Adsorption of arsenate and arsenite by iron-treated activated carbon and zeolites: effects of pH, temperature, and ionic strength, J. Environ. Sci. Health A Tox Hazard. Subst. Environ. Eng., 40 (2005) 723–749.

[20] R.C. Vaishya and S.K. Gupta, Arsenic removal from groundwater by iron impregnated sand, J. Environ. Eng., 129 (2003) 89–92.

[21] Y. Li, F.S. Zhang and F.R. Xiu, Arsenic (V) removal from aqueous system using adsorbent developed from a high iron-containing fly ash, Sci. Total Environ., 407 (2009) 5780–5786.

[22] H. Genc-Fuhrman, J.C. Tjell and D. McConchie, Adsorption of arsenic from water using activated neutralized red mud, Environ. Sci. Technol., 38 (2004) 2428–2434.

[23] H. Genc, J.C. Tjell, D. McConchie and O. Schuiling, Adsorption of arsenate from water using neutralized red mud, J. Colloid Interf. Sci., 264 (2003) 327–334.

[24] S. Zhang, C. Liu, Z. Luan, X. Peng, H. Ren and J. Wang, Arsenate removal from aqueous solutions using modified red mud, J. Hazard. Mater., 152 (2008) 486–492.

[25] S.R. Kanel, H. Choi, J.Y. Kim, S. Vigneswaran and W.G. Shim, Removal of arsenic(III) from groundwater using low-cost industrial by-products-blast furnace slag, Wat. Qual. Res. J. Canada, 41 (2006) 130–139.

[26] C. Jing, X. Meng, E. Calvache and G. Jiang, Remediation of organic and inorganic arsenic contaminated groundwater using a nanocrystalline TiO_2-based adsorbent, Environ. Pollut., 157 (2009) 2514–2519.

[27] S. Chakravarty, V. Dureja, G. Bhattacharyya, S. Maity and S. Bhattacharjee, Removal of arsenic from groundwater using low cost ferruginous manganese ore, Wat. Res., 36 (2002) 625–632.

[28] P.K. Dutta, A.K. Ray, V.K. Sharma and F.J. Millero, Adsorption of arsenate and arsenite on titanium dioxide suspensions, J. Colloid Interf. Sci., 278 (2004) 270–275.

[29] Y. Seida and Y. Izumi, Synthesis of clay–cerium hydroxide conjugates for the adsorption of arsenic, Adsorp. Sci. Technol., 23 (2005) 607–618.

[30] Y.H. Xu, T. Nakajima and A. Ohki, Adsorption and removal of arsenic(V) from drinking water by aluminum-loaded Shirasu-zeolite, J. Hazard. Mater., 92 (2002) 275–287.

[31] C.L. Guo, F.X. Zhang and X.Y. Yang, A study on the treatment of As-containing waste water by lime-polyferric sulphate coagulating process, Indust. Wat. Treat., 20 (2000) 27–29 (in Chinese with abstract in English).

[32] S. Bang, M. Patel, L. Lippincott and X. Meng, Removal of arsenic from groundwater by granular titanium dioxide adsorbent, Chemosphere, 60 (2005) 389–397.

[33] H. Sun, X. Zhang, Z. Zhang, Y. Chen and J.C. Crittenden, Influence of titanium dioxide nanoparticles on speciation and bioavailability of arsenite, Environ. Pollut., 157 (2009) 1165–1170.

[34] K. Gupta and U.C. Ghosh, Arsenic removal using hydrous nanostructure iron(III)–titanium(IV) binary mixed oxide from aqueous solution, J. Hazard. Mater., 161 (2009) 884–892.

[35] O.S. Thirunavukkarasu, T. Viraraghavan and K.S. Subramanian, Arsenic removal from drinking water using iron oxide-coated sand, Water, Air, Soil Pollut., 142 (2003) 95–111.

[36] C.D. Wagner, W.M. Riggs, L.E. Davis and J.F. Moulder, Handbook of X-ray Photoelectron Spectroscopy, Physical Electronics Division, Perkin-Elmer Corp, Eden Prairie, MN, 1979.

[37] V.K. Gupta, V.K. Saini and N. Jain, Adsorption of As(III) from aqueous solutions by iron oxide-coated sand, J. Colloid Interf. Sci., 288 (2005) 55–60.

[38] S. Kundu and A.K. Gupta, Adsorption characteristics of As(III) from aqueous solution on iron oxide coated cement (IOCC), J. Hazard. Mater., 142 (2007) 97–104.

[39] J.C. Hsu, C.J. Lin, C.H. Liao and S.T Chen, Removal of As(V) and As(III) by reclaimed iron-oxide coated sands, J. Hazard. Mater., 153 (2008) 817–826.

[40] S. Goldberg and C.T. Johnston, Mechanisms of arsenic adsorption on amorphous oxides evaluated using macroscopic measurements, vibrational spectroscopy, and surface complexation modeling, J. Colloid Interf. Sci., 234 (2001) 204–216.

[41] S.E. O'Reilly, D.G. Strawn and D.L. Sparks, Residence Time Effects on Arsenate Adsorption/Desorption Mechanisms on Goethite, 2001, pp. 67–77.

[42] H.S. Altundogan, S. Altundogan, F. Tumen and M. Bildik, Arsenic adsorption from aqueous solutions by activated red mud, Waste Manage., 22 (2002) 357–363.

[43] S. Wang, Y. Boyjoo, A. Choueib and Z.H. Zhu, Removal of dyes from aqueous solution using fly ash and red mud, Wat. Res., 39 (2005) 129–138.

[44] H. Genc-Fuhrman, H. Bregnhoj and D. McConchie, Arsenate removal from water using sand-red mud columns, Wat. Res., 39 (2005) 2944–2954.

[45] S. Goldberg, Competitive Adsorption of Arsenate and Arsenite on Oxides and Clay Minerals, 2002, pp. 413–421.